

# Design of advanced automotive exhaust catalysts

Hideaki Muraki\*, Geng Zhang

*Johnson Matthey Japan Incorporated, 5123-3, Kitsuregawa, Shioya-gun, Tochigi 329-1412, Japan*

## Abstract

Rhodium (Rh) is a critical component of current automotive three-way catalysts (TWCs), particularly with regard to  $\text{NO}_x$  and CO conversion at rich and stoichiometric air–fuel ratios (A/F). Rh supported on  $\text{CeO}_2$  was active for  $\text{NO}_x$  and CO conversions but could be deactivated easily by high temperature aging. The cause of the deactivation is ascribed to the sintering of  $\text{CeO}_2$ .  $\text{ZrO}_2$  incorporation into  $\text{CeO}_2$  is reported to have high thermal durability in terms of oxygen storage capacity (OSC). There has been no report showing direct experimental evidence that Rh-loaded on  $\text{CeO}_2$ – $\text{ZrO}_2$  mixed oxides induced effects on TWC performance improvement in the actual automotive exhaust. In the present paper, the Rh– $\text{CeO}_2$  interaction contributing to  $\text{NO}_x$  reduction and the catalytic behavior of Rh-loaded  $\text{CeO}_2$ – $\text{ZrO}_2$  mixed oxide is addressed. Incorporating  $\text{CeO}_2$ – $\text{ZrO}_2$  into a catalyst offered significant improvement in light-off and warmed-up performances in model gas test. Newly designed TWC including the Rh/ $\text{CeO}_2$ – $\text{ZrO}_2$  component were aged and evaluated on an engine dynamometer. Result of engine dynamometer evaluation also revealed that significant improvement in the thermal durability can be achieved by the utilization of the optimized Rh-loaded  $\text{CeO}_2$ – $\text{ZrO}_2$  mixed oxide. © 2000 Elsevier Science B.V. All rights reserved.

**Keywords:** Ceria; Ceria–zirconia; Rhodium; Three-way catalyst; Automotive exhaust

## 1. Introduction

Advanced automotive emission control technology in conjunction with sophisticated vehicle emission systems will be inevitable in helping to achieve improved global air quality. With a view to improving the activity and durability of catalyst technologies, alternative catalyst control strategies such as increasing platinum group metal (PGM) loading and increasing catalyst volume are possible approaches. An alternative approach to higher PGM loading is to improve catalytic activity by way of catalyst design. Significant performance improvements in three-way catalyst (TWC) formulations have been previously achieved by incorporating base metal promoters such as cerium (Ce) into TWC formulations. Ce in current ceria–alumina TWC formulations significantly

enhances  $\text{NO}_x$  and CO performance at near stoichiometric air/fuel ratios (A/F) [1–3].

Catalyst containing platinum group metal (PGM, Pt, Pd, Rh, etc.) and ceria as the support or additive have gained considerable importance because of their application in automotive pollution control and in syngas conversion. High temperature reduction of such catalysts in hydrogen induces enhanced interaction between metal and ceria and modifies drastically the catalytic activity [4–8]. Several models were proposed to account for this phenomenon but conclusive explanation is still lacking.

The behavior of Rh catalyst supported on ceria is of interest in view of its marvelous TWC performance in fresh. The contribution of  $\text{CeO}_2$  presence in a catalyst to the improvement of catalytic activity of TWC has been studied by many researchers [1,2,9–11]. The primary function of ceria in TWC is to provide oxygen storage capacity (OSC) in order to allow the catalyst

\* Corresponding author.

to operate over a wider range of air/fuel ratios (A/F) [12]. There was no researcher interested in the utilization of the property of Rh/CeO<sub>2</sub> in the design of TWC.

On the other hand, it has been reported that adding ZrO<sub>2</sub> to CeO<sub>2</sub> increase OSC [13], and stabilizes CeO<sub>2</sub> particles against thermal sintering [14]. While there have been extensive investigations [15–18] of the phase diagram and the redox behavior of the ceramic system and PGM loaded system CeO<sub>2</sub>–ZrO<sub>2</sub>, respectively, because of its electroconductive and mechanical properties, TWC performance of Rh/CeO<sub>2</sub>–ZrO<sub>2</sub> catalyst has not been reported.

In order to advance the design of automotive catalyst for maximum durability performance, the present study revealed the Rh–CeO<sub>2</sub> interaction contributes to NO<sub>x</sub> reduction. This allowed the utilization of CeO<sub>2</sub>–ZrO<sub>2</sub> mixed oxide as a support of Rh because of its thermal stability. Two newly designed TWCs containing the optimized Rh/CeO<sub>2</sub>–ZrO<sub>2</sub> component were evaluated in comparison with current high performance TWC.

## 2. Experimental

### 2.1. Laboratory reactor studies

To prepare the catalyst samples, Rh nitrate solution was deposited on ceria, alumina or CeO<sub>2</sub>–ZrO<sub>2</sub> mixed oxides powder by incipient wetness method. CeO<sub>2</sub>–ZrO<sub>2</sub> materials used in the paper are all commercially available and the surface areas of Rh supported CeO<sub>2</sub>–ZrO<sub>2</sub> are presented in Table 1. The resulted powder was then dried at 110°C overnight followed by calcination at 500°C for 2 h. The calcined powder was then blended with the same amount of alumina to make a washcoat slurry. The Rh content in the slurry was 0.20 wt.% for all catalysts used for model gas test. The complete catalysts are hereafter referred to Rh/CeZrXX where XX stands for the content in weight percent of CeO<sub>2</sub> in CeO<sub>2</sub>–ZrO<sub>2</sub>.

Table 1

Specific surface areas of fresh and 900°C redox aged Rh/CeO<sub>2</sub>–ZrO<sub>2</sub> catalysts

| Catalyst CeO <sub>2</sub> content (wt.%)     | Fresh (m <sup>2</sup> /g) | 900°C aged (m <sup>2</sup> /g) |
|--|---------------------------|--------------------------------|
| 10% CeO <sub>2</sub> (Rh/CeZr10)             | 49                        | 33                             |
| 20% CeO <sub>2</sub> (Rh/CeZr20)             | 57                        | 41                             |
| 30% CeO <sub>2</sub> (Rh/CeZr30)             | 83                        | 33                             |
| 57% CeO <sub>2</sub> (Rh/CeZr57)             | 109                       | 23                             |
| 66% CeO <sub>2</sub> (Rh/CeZr66)             | 97                        | 29                             |
| 100% CeO <sub>2</sub> (Rh/CeO <sub>2</sub> ) | 102                       | 37                             |

The washcoats obtained above were coated on 1.01 ceramic substrate with 400 cells per square inch cell density and 0.006 in. wall thickness and Rh loading was 0.35 g/l. A representative cylindrical core with 1 in. diameter and 30 mm long was drilled off from each catalyst block and loaded into an aging apparatus which consisted of a quartz tube surrounded by a Lindberg furnace. The aging apparatus was connected to a gas delivery system allowing the catalysts to be exposed to oxidative and reductive gases alternatively. The aging atmosphere was switched between oxidative and reductive gas compositions every 10 min at a space velocity of 2100 h<sup>−1</sup>. This aging method is referred to redox aging in the present paper. The gas compositions are as follows:

Oxidative gas composition — O<sub>2</sub> 3%, H<sub>2</sub>O 10%, N<sub>2</sub> balance.

Reductive gas composition — H<sub>2</sub> 6%, H<sub>2</sub>O 10%, N<sub>2</sub> balance.

The catalysts prepared were evaluated under dynamic conditions at a space velocity of 100 000 h<sup>−1</sup>. The reaction gas composition was switched between rich and lean as shown in Table 2 at a frequency of 1 Hz and an amplitude of ±0.6 A/F. Before measuring the light-off performance, pre-conditioning was performed in the following manner. The catalyst was heated up until 500°C and kept for 10 min at 500°C in the gas composition and cooled down to below 80°C

Table 2

Gas compositions for dynamic model gas test

| Dynamics | Gas composition |                    |                    |          |                                       |                                       |                     |                      |                |
|----------|-----------------|--------------------|--------------------|----------|---------------------------------------|---------------------------------------|---------------------|----------------------|----------------|
|          | CO (%)          | O <sub>2</sub> (%) | H <sub>2</sub> (%) | NO (ppm) | C <sub>3</sub> H <sub>6</sub> (ppm C) | C <sub>3</sub> H <sub>8</sub> (ppm C) | CO <sub>2</sub> (%) | H <sub>2</sub> O (%) | N <sub>2</sub> |
| Rich     | 2.11            | 0.50               | 0.70               | 500      | 900                                   | 300                                   | 14                  | 10                   | Balance        |
| Lean     | 0.50            | 1.54               | 0.17               | 500      | 900                                   | 300                                   | 14                  | 10                   | Balance        |

in the same model gas composition. The catalyst inlet temperature was raised to 500°C at 25°C/min in the gas composition. The concentrations of hydrocarbon, CO and NO<sub>x</sub> at the inlet and outlet of the reactor were collected for calculation of the conversions. The catalytic activities under warmed-up conditions were presented by the conversion at 400°C taken during light-off test.

## 2.2. Dynamometer reactor studies

Catalysts for the dynamometer reactor test were prepared by coating washcoat slurry on a 1.0 litre ceramic substrate with 400 cells per square inch cell density and 0.006 in wall thickness. Bench aging was carried out on a 4.0 litre V8 engine using sulfur contained fuel (S: 300 ppm) operating at stoichiometric air/fuel ratio which was utilized to produce accelerated catalyst deactivation.

The performance of aged catalysts was evaluated as a function of air/fuel ratio (A/F) (perturbed  $\pm 1$  A/F at 1 Hz of frequency) with a 2.0 litre L4 engine and the evaluation was performed at a space velocity of 60 000 h<sup>-1</sup>. The A/F was moved in discrete steps, starting at 15.5 and progressing in the rich direction to 14.0 A/F. At each new A/F setpoint, the conversion was allowed to stabilize for 5 min and then recorded. CO/NO<sub>x</sub> and THC/NO<sub>x</sub> cross-over points (COP) were determined from the plot of conversion efficiencies as a function of A/F. The light-off performance was also measured using the same engine conditions at the stoichiometric A/F by using a heat exchanger to raise the inlet temperature at 10°C/min.

## 2.3. BET surface area measurement of the samples

Specific surface area of samples was determined by physisorption of nitrogen at liquid nitrogen temperature using a Micromeritics Gemini 2370.

## 2.4. CO-TPR measurement

Catalyst sample of 0.10 g was placed in a quartz tube reactor through which 50 cm<sup>3</sup>/min of 2% CO/He was supplied continuously during the TPR measurement. The temperature was raised at a rate of 10°C/min from 50 to 800°C. Prior to the TPR, the catalyst was

pre-oxidized in 10% O<sub>2</sub>/He at 500°C for 15 min. The gas composition sampled at the outlet of the reactor was analyzed by a quadruple mass spectrometer. Argon gas, which is premixed with CO, was used as an internal standard for quantitative analysis.

# 3. Results and discussion

## 3.1. Effect of CeO<sub>2</sub> on NO<sub>x</sub> reduction activity of Rh

Ceria is used as a support for PGM in reactions other than automotive TWC, e.g., Pt–ceria for carbon monoxide hydrogenation [19], Rh–ceria for the decomposition of N<sub>2</sub>O [20]. As the superior action of ceria in these catalysts is often derived through the combination with PGM, knowledge of the interaction between ceria and PGM is critical to fully utilize the performance of both elements in designing efficient catalysts. However, there are discrepancies among the literatures concerning whether PGM aggregate on the surface of ceria or interact with it strongly so as to penetrate inside the bulk ceria. In order to develop a highly active TWC, it is necessary to design the catalyst with understanding of the effect of PGM–ceria interaction.

In order to demonstrate the effect of ceria on NO<sub>x</sub> reduction activity of Rh catalyst, the light-off performance and the warmed-up conversion of fresh Rh/CeO<sub>2</sub> catalyst was evaluated compared with those of fresh Rh/Al<sub>2</sub>O<sub>3</sub> catalyst.

The light-off performance at stoichiometric A/F under dynamic conditions is shown as a function of temperature in Fig. 1. Rh/CeO<sub>2</sub> catalyst shows an excellent light-off performance compared with Rh/Al<sub>2</sub>O<sub>3</sub> catalyst. Fig. 2 presents the warmed-up activities of both Rh/CeO<sub>2</sub> and Rh/Al<sub>2</sub>O<sub>3</sub> catalysts at 400°C under dynamic conditions. The result indicates that Rh/CeO<sub>2</sub> catalyst has better HC, CO, and NO<sub>x</sub> conversions than Rh/Al<sub>2</sub>O<sub>3</sub> catalyst. The difference in TWC performance between Rh/CeO<sub>2</sub> and Rh/Al<sub>2</sub>O<sub>3</sub> catalysts result from the presence of interaction between Rh and ceria.

The light-off performance and 400°C warmed-up conversions of both Rh/CeO<sub>2</sub> and Rh/Al<sub>2</sub>O<sub>3</sub> catalysts after 900°C, 20 h redox aging are presented in Figs. 3 and 4. The light-off performance of Rh/CeO<sub>2</sub> catalyst became slightly worse than that of Rh/Al<sub>2</sub>O<sub>3</sub> catalyst,

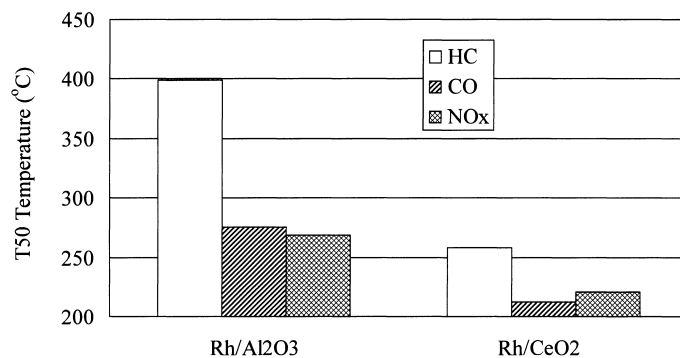


Fig. 1. Light-off temperatures under dynamic conditions on fresh Rh/Al<sub>2</sub>O<sub>3</sub> and Rh/CeO<sub>2</sub> catalysts.

while the warmed-up conversions of Rh/CeO<sub>2</sub> catalyst was still better than that of Rh/Al<sub>2</sub>O<sub>3</sub> catalyst except for HC conversion. That is, Rh/CeO<sub>2</sub> catalyst maintains the Rh–CeO<sub>2</sub> interaction to some extent so that

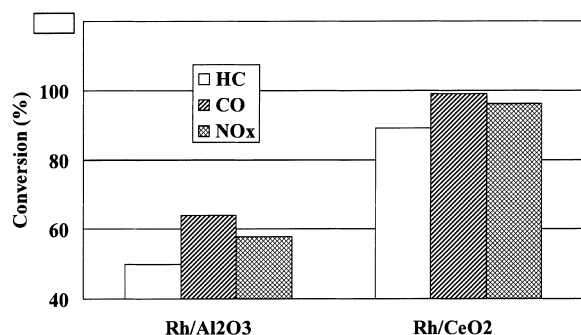


Fig. 2. Warmed-up conversions under dynamic conditions at 400°C on fresh Rh/Al<sub>2</sub>O<sub>3</sub> and Rh/CeO<sub>2</sub> catalysts.

it can contribute to NO<sub>x</sub> reduction and CO oxidation even after the aging. However, it is pointed out that the declines in light-off performance and warmed-up activity on Rh/CeO<sub>2</sub> are drastic in contrast to that on Rh/Al<sub>2</sub>O<sub>3</sub>. This fact could be ascribed to the poor thermal durability of Rh–CeO<sub>2</sub> interaction in Rh/CeO<sub>2</sub>.

The results also indicate that Rh loaded on alumina had better HC conversion than Rh loaded on ceria but the warmed up CO and NO<sub>x</sub> conversions of Rh loaded on alumina was very poor. It is desirable that Rh should be loaded on both alumina and ceria at a suitable ratio to derive TWC performance from Rh. On the other hand, TWC usually consists of Pt, Pd, and Rh as active components. Rh is used in TWC because of its excellent activity for reduction of NO<sub>x</sub> to nitrogen with low ammonia formation, and Pt and Pd mainly contribute to oxidation of HC and CO. Thus, the notable role of Rh is its NO<sub>x</sub> reduction activity and a stronger and stable interaction between Rh and

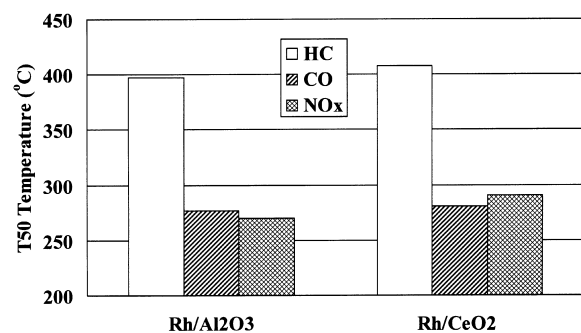


Fig. 3. Light-off temperatures under dynamic conditions on aged Rh/Al<sub>2</sub>O<sub>3</sub> and Rh/CeO<sub>2</sub> catalysts.

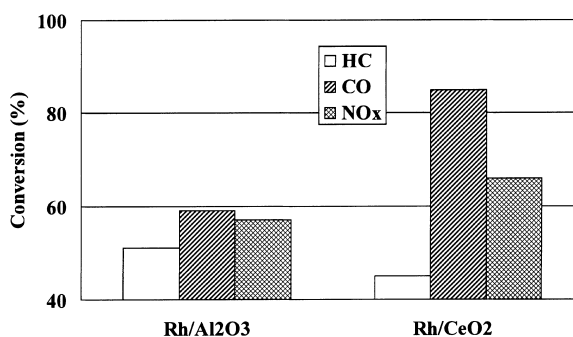


Fig. 4. Warmed-up conversions under dynamic conditions at 400°C on aged Rh/Al<sub>2</sub>O<sub>3</sub> and Rh/CeO<sub>2</sub>.

ceria is an inevitable issue in designing highly active advanced TWC.

Based on the consideration above, one of the keys to the development of advanced TWCs is the maintenance of the advantage of Rh–CeO<sub>2</sub> interaction even after high temperature aging. The dramatic deactivation of Rh/CeO<sub>2</sub> catalyst after the aging might result from the sintering of ceria.

One of the most important roles of CeO<sub>2</sub> in these Rh/CeO<sub>2</sub> systems is to act as oxygen storage/transport medium by shifting between Ce<sup>3+</sup> and Ce<sup>4+</sup> under reducing and oxidizing conditions, respectively. On the pure CeO<sub>2</sub>, it is reported reference that there is two kinds of oxygen available in CeO<sub>2</sub> to be reduced, i.e., the oxygen on CeO<sub>2</sub> surface and one in CeO<sub>2</sub> bulk [30]. The surface oxygen can be reduced much more readily than that inside CeO<sub>2</sub> bulk. Upon the addition of Rh on the CeO<sub>2</sub> surface, the reduction of surface oxygen becomes even faster [21]. At the same time, the transportation of oxygen from the bulk to the surface of CeO<sub>2</sub> is inhibited, probably, due to the occupation of oxygen vacancies by Rh. The same conclusion was drawn on Pt/CeO<sub>2</sub> system [22]. Therefore, the interaction between Rh and Ce is more an issue of the activity of surface oxygen than that in bulk of CeO<sub>2</sub>. An X-ray absorption analysis has confirmed the CeO<sub>2</sub> with high surface area would give quicker reduction of surface oxygen than that has lower surface area [21].

Therefore, the improvement of Rh–CeO<sub>2</sub> interaction could be achieved via two routes: (1) stabilization of the surface area of CeO<sub>2</sub> and CeO<sub>2</sub> particle size; (2) increase of oxygen mobility in CeO<sub>2</sub>. Recently, there are quite a few studies been done on the CeO<sub>2</sub> stabilization by introducing the foreign ion(s) into CeO<sub>2</sub> crystal lattice. For example, it was reported the redox properties were strongly enhanced if foreign cations such as Zr [14,23], Gd [24], Pr [25], Tb [26], and Pb [27] were introduced into the CeO<sub>2</sub> lattice by forming solid solutions. The improvement was the result of enhanced oxygen ion mobility inside the modified fluorite lattice originating from the formation of a defective, fluorite-structured solid solution in which cations of different radius and/or charge have replaced Ce atoms. Much effort has been focused on the preparation of these mixed oxides, which are potentially useful as catalysts for sensors, for carrying out selective oxidation, and for providing low ignition temperatures for catalyzed combustion process.

Also, a great number of systems have been examined with the view to increasing the thermal stability of CeO<sub>2</sub> and preventing decline of OSC. Addition of ZrO<sub>2</sub> to CeO<sub>2</sub> significantly increases the thermal stability of CeO<sub>2</sub> and improves its ability to store and release oxygen (OSC) under reaction conditions [28]. Characterization using Pulsed Neutron Scattering method has suggested that the phase segregation in a nanometer scale was the origin of the high OSC from CeO<sub>2</sub>–ZrO<sub>2</sub> [29]. In another word, CeO<sub>2</sub> existing as nanometer size particle inside CeO<sub>2</sub>–ZrO<sub>2</sub> offers the highly thermally durable OSC.

Based on the results above, supporting Rh on carefully prepared CeO<sub>2</sub>–ZrO<sub>2</sub> is expecting to provide stable Rh–CeO<sub>2</sub> interaction, which is responsible for TWC performance.

There is no report, which uses Rh/CeO<sub>2</sub>–ZrO<sub>2</sub> in actual TWC application so far to our knowledge. In the next section, we have examined by model gas test the activity of Rh supported on several kinds of CeO<sub>2</sub>–ZrO<sub>2</sub> with varied CeO<sub>2</sub> content in comparison to Rh/CeO<sub>2</sub> catalyst.

### 3.2. Evaluation of Rh/CeO<sub>2</sub>–ZrO<sub>2</sub> catalyst

Following 900°C, 20 h redox aging, the light-off performance of five Rh/CeO<sub>2</sub>–ZrO<sub>2</sub> catalysts is shown in Fig. 5. Obviously, all catalysts using CeO<sub>2</sub>–ZrO<sub>2</sub> have improved light-off and warmed-up activity as compared to Rh/CeO<sub>2</sub>. The light-off performance of Rh/CeZr10, Rh/CeZr20 and Rh/CeZr66 that contain 10, 20 and 66% of CeO<sub>2</sub> in CeO<sub>2</sub>–ZrO<sub>2</sub>, respectively, were the best and that of Rh/CeZr57

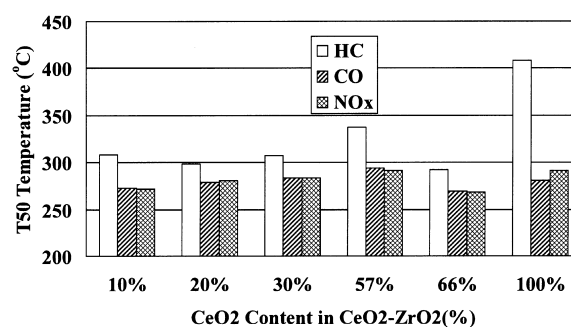


Fig. 5. Effect of ceria concentration on light-off temperature under dynamic conditions on aged Rh catalysts.

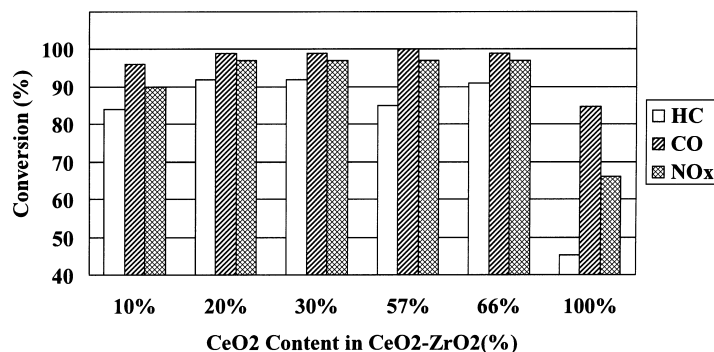


Fig. 6. Effect of ceria concentration on warmed-up conversions under dynamic conditions at 400°C on aged Rh catalysts.

was the worst among those of five catalysts. Fig. 6 presents the warmed-up conversions at 400°C of aged Rh/CeO<sub>2</sub>-ZrO<sub>2</sub> catalysts. The CO and NO<sub>x</sub> conversions are in the order as follows: CeZr57 > CeZr20 = CeZr30 = CeZr66 > CeZr10 > CeO<sub>2</sub>. The promoting effect of Zr on CeO<sub>2</sub> is significant from these results. As the activities for CO and NO<sub>x</sub> are strongly related to OSC of the material used, the observation in Figs. 5 and 6 clearly indicates that ZrO<sub>2</sub>-CeO<sub>2</sub>s have improved thermal durability of OSC as compared to pure CeO<sub>2</sub>. The light-off temperatures of HC and NO<sub>x</sub> of fresh and aged Rh/CeO<sub>2</sub>-ZrO<sub>2</sub> catalyst were also compared in Fig. 7. From this figure, it is noted that the deactivation of light-off performances is most serious for pure CeO<sub>2</sub> supported Rh and followed by Rh on CeZr30. Therefore, the stabilization of Rh-Ce interaction is attained in CeZr20 and CeZr66 more successfully than on the

other CeO<sub>2</sub>-ZrO<sub>2</sub> such as CeZr30. XRD analysis also revealed some portion of Zr existed in CeZr30 as isolated ZrO<sub>2</sub> rather than as CeO<sub>2</sub>-ZrO<sub>2</sub> solid solution. Interestingly, Rh/CeZr20 has shown the comparable activity to Rh/CeZr66 in spite of the low content of CeO<sub>2</sub> in CeZr20.

Table 1 compares BET surface areas of Rh/Ce-Zr catalysts in fresh and after 900°C, 20 h redox aging. The surface area of fresh catalysts increases with CeO<sub>2</sub> content. Following 900°C redox aging, there was not significant difference in surface area among Rh/CeO<sub>2</sub>-ZrO<sub>2</sub> tested except for Rh/CeZr57 catalyst. The difference in the surface area of Rh/CeO<sub>2</sub>-ZrO<sub>2</sub> catalyst after aging could not explain the data shown in Figs. 5–7 satisfactorily.

Fig. 8 presents the CO<sub>2</sub> formation with increase in temperature during CO-TPR with aged Rh/CeZr20 and Rh/CeZr66 which are the best Rh/CeO<sub>2</sub>-ZrO<sub>2</sub> tested in this paper. The peaks appearing at temperature below 400°C could be assigned to the oxygen located on the surface of Rh/CeO<sub>2</sub>-ZrO<sub>2</sub> and the CO<sub>2</sub> generated at higher temperature region to those from bulk CeO<sub>2</sub> [25,30–32]. Obviously, CeZr66 has more oxygen available than CeZr20, especially at the temperature higher than 400°C. It could be concluded that almost all oxygen, which is available on CeZr20, is associated with CO<sub>2</sub> formation at low temperature region while significant portion of oxygen which is available on CeZr66 is from bulk CeO<sub>2</sub>. It is generally accepted that the oxygen available at lower temperature possesses higher catalytic activity than those available at higher temperature. The equivalent amount of oxygen, which is active at below 400°C in CeZr20

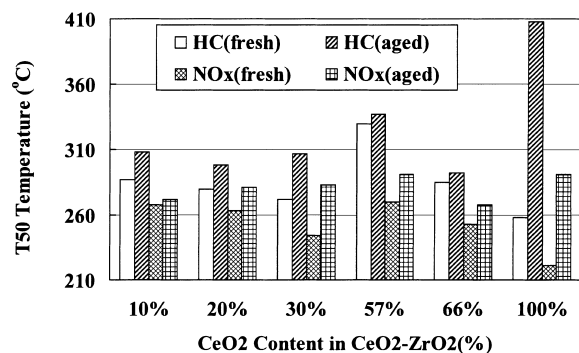


Fig. 7. Effect of ceria concentration on light-off temperature under dynamic conditions on fresh and aged Rh catalysts.

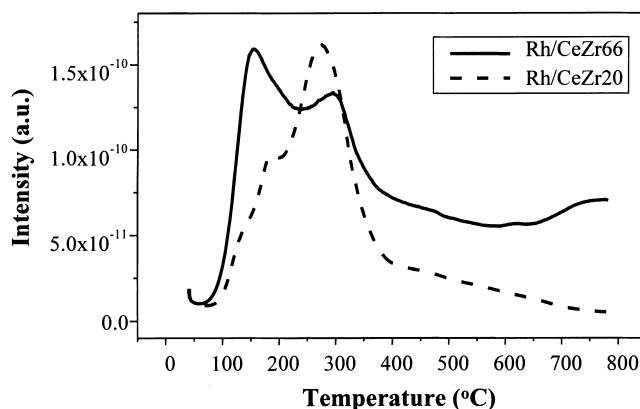


Fig. 8. CO-TPR profiles of Rh/CeZr20 and Rh/CeZr66 after aging.

to that in CeZr66, could explain its high activity as shown in Figs. 5 and 6 irrespective to its low CeO<sub>2</sub> content.

Based on the TPR results, it appears that all OSC in Rh/CeZr20 is associated with Rh–CeO<sub>2</sub> interaction. As we are more interested in the effectiveness of OSC originated from Rh–CeO<sub>2</sub> interaction on a catalyst surface on TWC performance, CeZr20 is selected as the material for further investigation in the following section.

### 3.3. Effectiveness of Rh–Ce interaction in the actual TWCs

In order to advance the design of TWC for maximum durability performance, it is important to maintain the advantage of Rh–CeO<sub>2</sub> interaction even after

high temperature aging. Rh/CeO–ZrO<sub>2</sub> is incorporated into the two typical TWC systems, i.e., Pt/Rh and Pd/Rh systems, to confirm the effectiveness of the thermally durable Rh–CeO<sub>2</sub> interaction for TWC application.

#### 3.3.1. Pt/Rh catalyst

Washcoat structure of an advanced Pt/Rh catalyst was manipulated for maintaining the interaction between Rh and CeO<sub>2</sub>–ZrO<sub>2</sub>. It contains the Rh/CeO<sub>2</sub>–ZrO<sub>2</sub> component in its structure. A current Pt/Rh catalyst was prepared without consideration of the interaction between Rh and CeO<sub>2</sub>–ZrO<sub>2</sub>. Pt/Rh ratio is 5/1 and the total PGM loading is 1.2 g/l.

Both catalysts were aged under the stoichiometric A/F conditions for 100 h and the inlet gas temperature is 850°C during the aging.

Fig. 9 displays the light-off performance of current and advanced Pt/Rh catalysts after 850°C, 100 h aging. Advanced catalyst had better light-off performance than current catalyst especially with respect to CO and NO<sub>x</sub>. This result indicates that advanced catalyst maintains the strong interaction between Rh and CeO<sub>2</sub> after the severe aging.

COP conversions of CO–NO<sub>x</sub>, THC–NO<sub>x</sub> and NO<sub>x</sub> conversion at A/F = 14.1 (rich A/F) are shown in Fig. 10. After 850°C aging, the advanced catalyst exhibited higher conversions than current catalyst. NO<sub>x</sub> conversion at rich A/F of advanced catalyst was extremely higher than that of current catalyst.

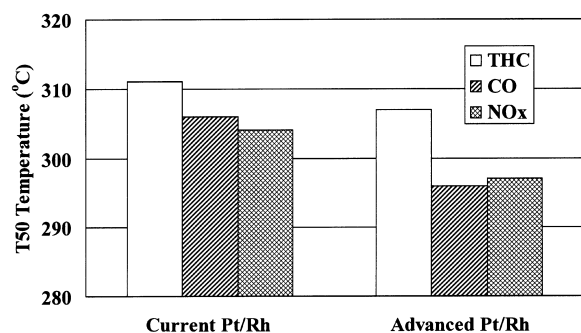


Fig. 9. Light-off performance of advanced and current Pt/Rh catalysts in engine exhaust gas after engine aging.

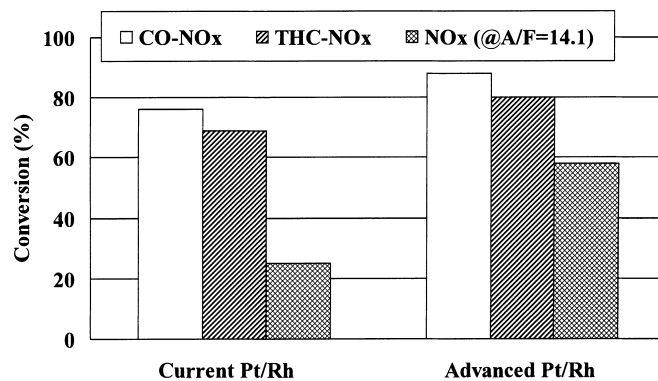


Fig. 10. COP and NO<sub>x</sub> conversions of advanced and current Pt/Rh catalysts at 350°C in engine exhaust gas after engine aging.

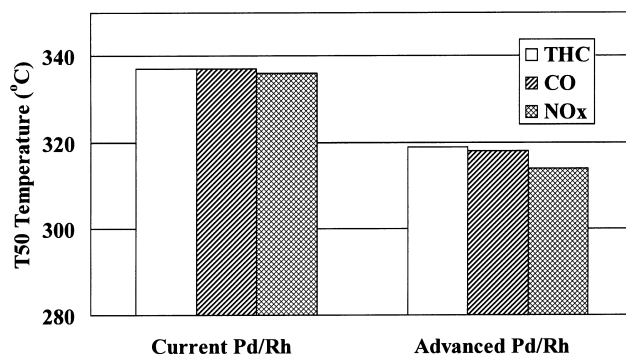


Fig. 11. Light-off performance of advanced and current Pd/Rh catalysts in engine exhaust gas after engine aging.

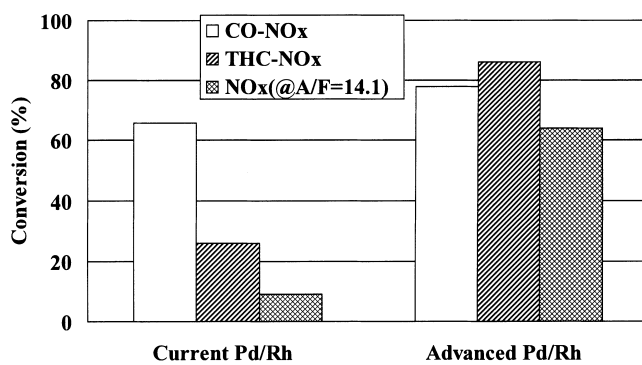


Fig. 12. COP and NO<sub>x</sub> conversions of advanced and current Pd/Rh catalysts at 400°C in engine exhaust gas after engine aging.



This fact could be explained by the high activity of water–gas-shift reaction contributed from strong Rh–CeO<sub>2</sub> interaction.

### 3.3.2. Pd/Rh catalyst

An advanced Pd/Rh TWC was also prepared using engineered washcoat technique for maintaining the property of Rh/CeO<sub>2</sub>–ZrO<sub>2</sub>. Pd/Rh ratio is 11/1 and the total PGM loading is 2.8 g/l. A current Pd/Rh catalyst was prepared by normal manner.

Current and the advanced catalysts were aged under the same condition as that for Pt/Rh described above. The evaluation of both aged catalysts was performed in the same way as that for the Pt/Rh catalysts.

Fig. 11 shows the light-off performance of current and advanced Pd/Rh catalysts after aging. Advanced catalyst had better light-off temperature than current Pd/Rh catalyst. Fig. 12 displays the COP conversions of CO–NO<sub>x</sub>, THC–NO<sub>x</sub> and NO<sub>x</sub> conversion at A/F = 14.1. Fig. 12 indicates that advanced catalyst had extremely higher COP conversion of THC–NO<sub>x</sub> and NO<sub>x</sub> conversion at A/F = 14.1 compared with current catalyst. The effectiveness of strong Rh–CeO<sub>2</sub> interaction is confirmed again in the Pd/Rh system.

## 4. Conclusions

Fresh Rh/CeO<sub>2</sub> showed excellent reduction activity of NO<sub>x</sub> in model gas test but deactivated significantly by thermal aging. Rh–CeO<sub>2</sub> is considered to play important role in the fresh Rh/CeO<sub>2</sub>. It was found introduction of Zr into CeO<sub>2</sub> crystal lattice could help significantly the stabilization of Rh–CeO<sub>2</sub> interaction via, probably, improving mobility of oxygen in CeO<sub>2</sub> or maintain CeO<sub>2</sub> dispersion in nanometer scale. The utilization of CeO<sub>2</sub>–ZrO<sub>2</sub> as Rh support in actual TWC proved CeO<sub>2</sub>–ZrO<sub>2</sub> is a useful material for practical TWC application.

## Acknowledgements

The authors would like to thank the Johnson Matthey Product Development Groups and Catalyst Evaluation Teams at KITEC, Japan and also Johnson Matthey plc for permission to publish this paper.

## References

- [1] G. Kim, *Ind. Eng. Chem. Prod. Res. Dev.* 21 (1982) 267.
- [2] B.J. Cooper, T.J. Truex, *SAE Paper* 850128 (1985).
- [3] W.B. Williamson, J.C. Summers, J.F. Skowron, *SAE Transactions Paper* 880103, 97 (1988) 341.
- [4] S.J. Tauster, S.C. Fung, *J. Catal.* 55 (1978) 29.
- [5] P. Meriaudeau, J.F. Dutel, M. Dufaux, C. Naccache, *Stud. Surf. Sci. Catal.* 11 (1982) 95.
- [6] G.S. Zafiris, R.J. Gorte, *J. Catal.* 139 (1993) 561.
- [7] M. Guenin, P.N. Da Silva, R. Fretty, *Appl. Catal.* 46 (1986) 313.
- [8] J.S. Rieck, A.T. Bell, *J. Catal.* 99 (1986) 278.
- [9] J.C. Summers, S.A. Ausen, *J. Catal.* 58 (1979) 131.
- [10] E.C. Su, C.N. Montreuil, W.G. Rothschild, *Appl. Catal.* 17 (1985) 75.
- [11] D.R. Monroe, M.H. Krueger, *SAE Paper* 872130 (1987).
- [12] P. Loof, B. Kasemo, K.E. Keck, *J. Catal.* 118 (1989) 339.
- [13] T. Murota, T. Hasegawa, S. Aozasa, H. Matsui, M. Motoyama, *J. Alloys Compounds* 193 (1993) 298.
- [14] L.L. Murrell, S.J. Tauster, in: A. Crucq (Ed.), *Catalysis and Automotive Pollution Control II*, Elsevier, Amsterdam, 1991, p. 547.
- [15] P. Duwez, F. Odell, *J. Am. Ceram. Soc.* 33 (1950) 274.
- [16] E. Tani, M. Yoshimura, S. Somyia, *J. Am. Ceram. Soc.* 66 (1983) 506.
- [17] S. Meriani, G. Spinolo, *Power Diff.* 2 (1987) 255.
- [18] S. Meriani, *Mater. Sci. Eng.* A109 (1989) 121.
- [19] D.S. Kalakkad, A.K. Datye, H.J. Robota, *J. Catal.* 148 (1994) 729.
- [20] S. Imamura, N. Okamoto, Y. Saito, T. Ito, H. Jindai, *J. Jpn. Petro. Ins.* 39 (1996) 350.
- [21] J. ElFallah, S. Boujana, H. Dexpert, A. Kiennemann, J. Majerus, O. Touret, F. Villain, F. Le Normand, *J. Phys. Chem.* 98 (1998) 5522.
- [22] V.P. Zhdanov, B. Kasemo, *Appl. Surf. Sci.* 135 (1998) 297.
- [23] P. Fornasiero, R. Di Monte, G. Ranga Rao, J. Kaspar, S. Meriani, A. Trovarelli, M. Graziani, *J. Catal.* 151 (1995) 168.
- [24] B.K. Cho, *J. Catal.* 131 (1991) 74.
- [25] A.D. Logan, M. Shelef, *J. Mater. Res.* 9 (1994) 468.
- [26] F. Zamar, A. Trovarelli, C. de Leitenburg, G. Dolcetti, *Stud. Surf. Sci. Catal.* 101 (1996) 1283.
- [27] Y. Zhang, A. Andersson, M. Muhammed, *Appl. Catal. B* 6 (1995) 325.
- [28] Eur. Patent, EP337809, *Appl.* 18/10/1989; Ger. Offen., DE37377419, *Appl.* 19/5/1988.
- [29] T. Egami, W. Dmowski, R. Brezny, *SAE paper* 970461.
- [30] H.C. Yao, Y.-F. Yu Yao, *J. Catal.* 86 (1984) 254.
- [31] L.A. Bruce, M. Hoang, A.E. Hughes, T.W. Turney, *Appl. Catal. A* 134 (1996) 351.
- [32] E. Rogemond, R. Frety, V. Perricho, M. Primet, S. Salasc, M. Chevrier, G. Gauthier, F. Mathis, *J. Catal.* 169 (1997) 120.